Entanglement effects and dilepton rate.

Chowdhury Aminul Islam

Saha Institute of Nuclear Physics
Kolkata

20.11.15

Based on PRD 92, 096002 (2015) [arXiv:1508.04061]

CNT QGP Meet 2015, VECC

Outline:

- Introduction.
- Entanglement.
- Effective QCD models.
- Vector meson spectral function and dilepton rate.
- Conclusions.

- Introduction.
- Entanglement.
- Effective QCD models.
- Vector meson spectral function and dilepton rate.
- Conclusions.

- The very first prototype of QCD phase diagram: [Cabibbo & Parisi, PLB 59 (1975)]

QCD phase diagram

- The very first prototype of QCD phase diagram: [Cabibbo & Parisi, PLB 59 (1975)]

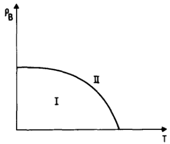

Fig. 1. Schematic phase diagram of hadronic matter. ρ_B is the density of baryonic number. Quarks are confined in phase I and unconfined in phase II.

QCD phase diagram

- The very first prototype of QCD phase diagram: [Cabibbo & Parisi, PLB 59 (1975)]

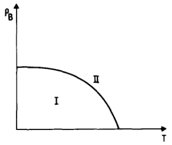

Fig. 1. Schematic phase diagram of hadronic matter. ρ_B is the density of baryonic number. Quarks are confined in phase I and unconfined in phase II.

- With the passage of time more and more investigations culminated in a very complicated looking phase diagram with many exotic phases: [Fukushima & Hatsuda, RPP 74 (2011)]

- The very first prototype of QCD phase diagram: [Cabibbo & Parisi, PLB 59 (1975)]

- With the passage of time more and more investigations culminated in a very complicated looking phase diagram with many exotic phases: [Fukushima & Hatsuda, RPP 74 (2011)]

QCD phase diagram

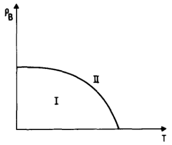

Fig. 1. Schematic phase diagram of hadronic matter. ρ_B is the density of baryonic number. Quarks are confined in phase I and unconfined in phase II.

QCD phase diagram

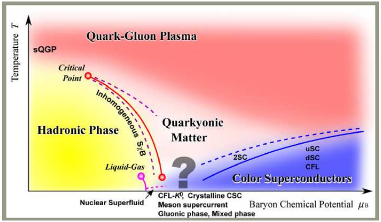

- The very first prototype of QCD phase diagram: [Cabibbo & Parisi, PLB 59 (1975)]

- With the passage of time more and more investigations culminated in a very complicated looking phase diagram with many exotic phases: [Fukushima & Hatsuda, RPP 74 (2011)]

QCD phase diagram

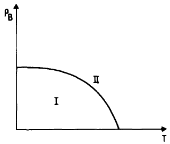

Fig. 1. Schematic phase diagram of hadronic matter. ρ_B is the density of baryonic number. Quarks are confined in phase I and unconfined in phase II.

QCD phase diagram

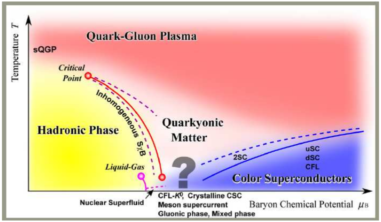

- Our interest will revolve around two phase transitions - chiral and deconfinement transitions.

- Introduction.
- Entanglement.
- Effective QCD models.
- Vector meson spectral function and dilepton rate.
- Conclusions.

- Chiral phase transition is defined in the vanishing quark mass limit, whereas the deconfinement phase transition in the quenched limit of infinite quark mass.
- The transitions are of first order in these limits.
- An important question is the nature of these phase transitions with the intermediate quark masses.
- Conceptually these two phase transitions are two distinct phenomena and, theoretically speaking, they reside in the opposite limits of quark masses.
- Lattice QCD (LQCD) simulations have confirmed the coincidence of these two transitions at the same temperature. [Fukugita & Ukawa PRL 57 (1986), Aoki et al PLB 643 (2006)]

- Is it a mere coincidence?
- The question was raised with the probable answer in the article, [Fukushima , PRD 77 (2008)].
- A strong entanglement (correlation) between the two phenomena was conjectured and investigate properly in the article, [Sakai *et al.*, PRD 82 (2010)].
- We take into account this entanglement effect and revist our earlier work, [Islam *et al.*, JHEP, 02 (2015)].

- Introduction.
- Entanglement.
- Effective QCD models.
- Vector meson spectral function and dilepton rate.
- Conclusions.

- Our work is based on effective QCD models, namely PNJL model and its entangled version.
- We can uniquely determine the coupling between the chiral condensate and the Polyakov loop.
- The Lagrangian we work with is the two flavour PNJL model with isoscalar-vector type interaction:

$$\begin{aligned}\mathcal{L}_{\mathrm{PNJL}} &= \bar{\psi}(i\gamma_\mu D^\mu - m)\psi + \frac{G_S}{2}[(\bar{\psi}\psi)^2 + (\bar{\psi}i\gamma_5\vec{\tau}\psi)^2] - \frac{G_V}{2}(\bar{\psi}\gamma_\mu\psi)^2 \\ &- \mathcal{U}[\Phi, \bar{\Phi}, T].\end{aligned}$$

- The corresponding thermodynamic potential for the PNJL model:

$$
\begin{aligned}
\Omega_{\mathrm{PNJL}} &= \mathcal{U}(\Phi, \bar{\Phi}, T) + \frac{G_S}{2}\sigma^2 - \frac{G_V}{2}n^2 \\
&- 2N_f T \int \frac{d^3p}{(2\pi)^3} \ln\left[1 + 3\left(\Phi + \bar{\Phi}e^{-(E_p-\tilde{\mu})/T}\right)e^{-(E_p-\tilde{\mu})/T} + e^{-3(E_p-\tilde{\mu})/T}\right] \\
&- 2N_f T \int \frac{d^3p}{(2\pi)^3} \ln\left[1 + 3\left(\bar{\Phi} + \Phi e^{-(E_p+\tilde{\mu})/T}\right)e^{-(E_p+\tilde{\mu})/T} + e^{-3(E_p+\tilde{\mu})/T}\right] \\
&- \kappa T^4 \ln[J(\Phi, \bar{\Phi})] - 2N_f N_c \int_\Lambda \frac{d^3p}{(2\pi)^3} E_p
\end{aligned}
$$

- The coupling between the chiral condensate and the Polyakov loop is $\sim \Phi e^{-M/T}$.

- The strength of the coupling is not strong enough to make the two transitions coincide within the range given by LQCD ($T_\sigma \approx T_\Phi \approx 173 \pm 8$ MeV). [Karsch et al NPB 605 (2001)]

[Ratti et al PRD 73 (2006)]

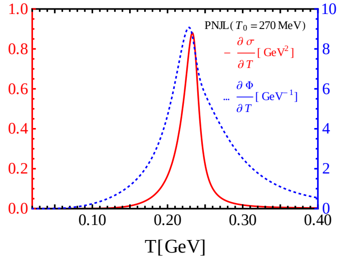

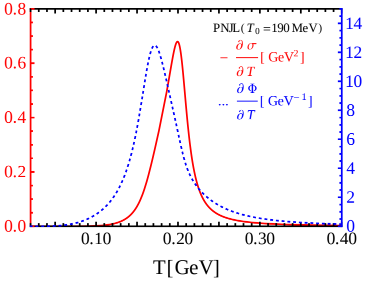

- Variations of $\frac{\partial\sigma}{\partial T}$ and $\frac{\partial\Phi}{\partial T}$ with temperature for different values of T_0. For $\mu = 0$, $\Phi = \bar{\Phi} = |\Phi|$.

- We introduce a stronger correlation through the entanglement between the two phenomena.

- The effective vertices are introduced through the ansatz:

$$\tilde{G}_S(\Phi) = G_S[1 - \alpha_1 \Phi\bar{\Phi} - \alpha_2(\Phi^3 + \bar{\Phi}^3)],$$ [Sakai *et al.*, PRD 82 (2010)]

and

$$\tilde{G}_V(\Phi) = G_V[1 - \alpha_1 \Phi\bar{\Phi} - \alpha_2(\Phi^3 + \bar{\Phi}^3)].$$ [Sugano *et al.*, PRD 90 (2014)]

- These ansatzes are guided by symmetry.

- α_1 and α_2 are two parameters in the EPNJL model, the values of which are to be fixed. We found $(\alpha_1, \alpha_2) = (0.1, 0.1)$.

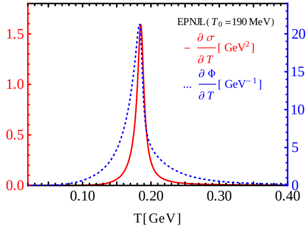

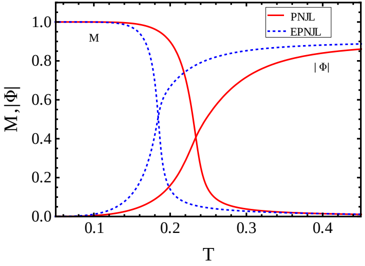

- Considerable change in the crossover transitions for both σ and Φ in EPNJL model as compared to the PNJL one.

- For $\mu = 0$, $\Phi = \bar{\Phi} = |\Phi|$.

PNJL

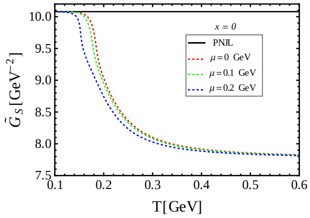

EPNJL

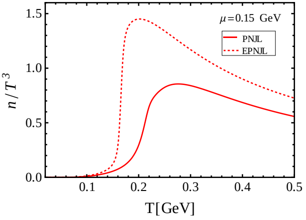

- $\tilde{G}_S$ in the EPNJL model becomes dependent on T and μ through Φ and thus runs.
- The quark number density rises very sharply for EPNJL model as compared to the PNJL one beyond 150 MeV.

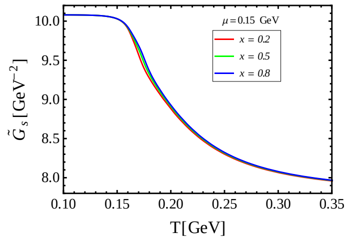

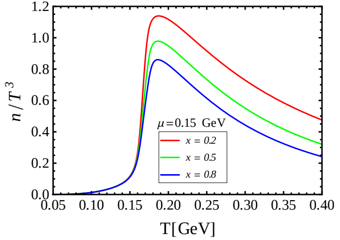

- As G_V is increased the value of $\tilde{G}_S$ increases.
- The quark number density decreases for a given temperature and chemical potential with the increase of G_V.

- Introduction.
- Entanglement.
- Effective QCD models.
- Vector meson spectral function and dilepton rate.
- Conclusions.

- Many properties of deconfined, strongly interacting matter are reflected in the structure of the correlation functions and its spectral representation.

- Thermal Current-Current Correlator in Eucledean time τ:

$$\mathcal{G}^E_M(\tau,\vec{x}) = \langle \mathcal{T}(J_M(\tau,\vec{x})J^\dagger_M(0,\vec{0}))\rangle_\beta$$

- τ is restricted to the interval $[0,\ \beta = 1/T]$ and $\omega_n = 2\pi n T$, $n = 0, 1, 2\cdots$

- The corresponding spectral function can be obtained through the analytic continution of $\mathcal{G}^E_M(\omega_n = \omega + i\epsilon)$:

$$\sigma_H(\omega,\vec{q}) \quad = \quad \frac{1}{\pi}\text{Im }\mathcal{G}^E_H(\omega + i\epsilon,\vec{q})$$

- $H = (00, ii, V)$ denotes (temporal, spatial, vector).

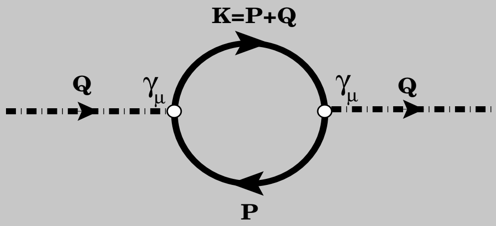

- The current-current correlator in vector channel at one loop level:

$$\Pi_{\mu\nu}(Q) = \int \frac{d^4P}{(2\pi)^4} \mathrm{Tr}_{D,c}\left[\gamma_\mu S(P+Q)\gamma_\nu S(P)\right]$$

- $\mathrm{Tr}_{D,c}$ is trace over Dirac and colour indices respectively.

- The PNJL effective quark propagator is given as:

$$S_{\mathrm{PNJL}}(L) = [\gamma_\mu L^\mu - M_f + \gamma_0\tilde{\mu} - i\gamma_0\mathcal{A}_4]^{-1}$$

- The four momentum $L \equiv (l_0, \vec{l})$.

- The distribution function can be generalised to PNJL through the relation:

$$f(E_p \pm \tilde{\mu}) = \frac{\Phi e^{-\beta(E_p\pm\tilde{\mu})} + 2\bar{\Phi}e^{-2\beta(E_p\pm\tilde{\mu})} + e^{-3\beta(E_p\pm\tilde{\mu})}}{1 + 3\Phi e^{-\beta(E_p\pm\tilde{\mu})} + 3\bar{\Phi}e^{-2\beta(E_p\pm\tilde{\mu})} + e^{-3\beta(E_p\pm\tilde{\mu})}}$$

[Hansen *et al.*, PRD 75 (2007)]

- We have studied the properties of the vector meson current-current correlation function with and without the isoscalar-vector interaction.

- The influence of isoscalar-vector interaction on the vector meson correlator is obtained using the ring approximation(RPA). [Davidson *et al.*, PLB 359 (1995), zero temp.]

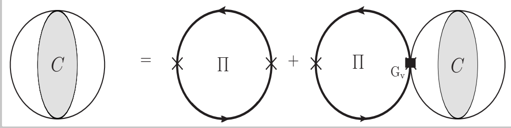

- The coupling constant G_V, which is considered to be a free parameter (as can't be fitted) in our calculation, comes into the picture.

- The DSE for $C_{\mu\nu}$ within ring summation:

$$C_{\mu\nu} = \Pi_{\mu\nu} + G_V \Pi_{\mu\sigma} C^{\sigma}_{\nu},$$

where $\Pi_{\mu\nu}$ is one loop vector correlator.

- The general structure of the resummed vector correlator in medium reads [Islam *et al.*, JHEP, 02 (2015)]:

$$C_{\mu\nu} = \frac{\Pi_T}{1 - G_V \Pi_T} P^T_{\mu\nu} + \frac{\Pi_L}{1 - G_V \Pi_L} P^L_{\mu\nu},$$

$P^{L(T)}_{\mu\nu}$ are longitudinal (transverse) projecton operators.

- The resummed vector correlator:

$$C_{\mu\nu} = \frac{\Pi_T}{1 - G_V \Pi_T} A^T_{\mu\nu} + \frac{\Pi_L}{1 - G_V \Pi_L} A^L_{\mu\nu}$$

- Corresponding resummed spectral function:

$$\sigma^R_V = \frac{1}{\pi}\Big[\mathrm{Im} C_{00} - \mathrm{Im} C_{ii}\Big].$$

- The imaginary parts (temporal & spatial) of one loop vector correlator are associated with an energy conserving delta function that imposes a finite limit of the quark loop momentum: $p_\pm = \frac{\omega}{2}\sqrt{1 - \frac{4M_f^2}{M^2}} \pm \frac{q}{2}$.

- For a given G_V and T, the resummed spectral function picks up continuous contribution above the threshold, $M^2 > 4M_f^2$.

- The differential dilepton production rate in terms of spectral function:

$$\frac{dR}{d^4x d^4Q} = \frac{5\alpha^2}{54\pi^2}\frac{1}{M^2}\frac{1}{e^{\omega/T}-1}\sigma_V(\omega,\vec{q})$$

with, $\alpha = \frac{e^2}{4\pi}$; $Q \equiv (q_0 = \omega, \vec{q})$ and $q = |\vec{q}|$, invariant mass $M = \sqrt{\omega^2 - q^2}$.

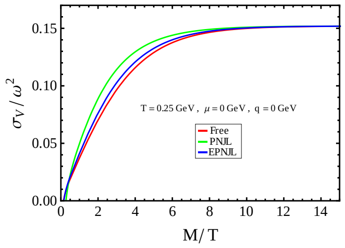

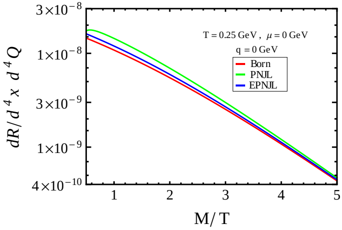

- At $\vec{q} = 0$ and $\mu_q = 0$ the spectral function is proportional to $[1 - 2f(E_p)]$, $f(E_p)$ is the fermion distribution function.
- Presence of Polyakov Loop $\rightarrow$ suppression in $f(E_p)$, hence enhancement in spectral function.
- The dilepton rate in EPNJL model is suppressed as compared to the PNJL one but is greater than the Born rate.

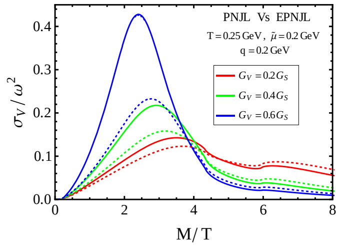

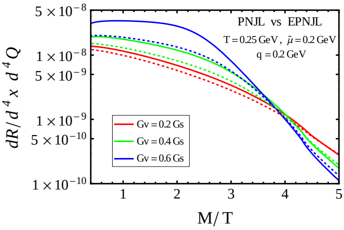

- At any value of G_V the strength of the spectral function for PNJL model is greater than that in the EPNJL one.
- As we increase G_V the difference between the two models becomes more prominent.
- The entanglement effect, overall, is more prominent than that with only the scalar-type interaction.

- Introduction.
- Entanglement.
- Effective QCD models.
- Vector meson spectral function and dilepton rate.
- Conclusions.

- The entanglement between σ & Φ leads to the coincidence between the two transitions.
- The entanglement effect relatively enhances the colour degrees of freedom due to the running of both the scalar (G_S) and vector (G_V) couplings.
- Vector meson spectral function in EPNJL model is suppressed as compared to the PNJL one in the region of low invariant mass.
- This suppression is reflected in the corresponding dilepton rates in PNJL and EPNJL models.

Collaborators:

- Sarbani Majumder
- Munshi Golam Mustafa

Thank You

Imaginary parts of the resummed vector correlator:

- The temporal component:

$$\mathrm{ImC}_{00} = \frac{\mathrm{Im}\Pi_{00}}{\left[1 - G_V\left(1 - \frac{\omega^2}{q^2}\right)\mathrm{Re}\Pi_{00}\right]^2 + \left[G_V(1 - \frac{\omega^2}{q^2})\mathrm{Im}\Pi_{00}\right]^2}$$

- The spatial component:

$$\mathsf{Im}C_{ii} = \mathsf{Im}C'_T + \mathsf{Im}C'_L,$$

$$\mathrm{Im}C'_T = \frac{\mathrm{Im}\Pi_{ii} - \frac{\omega^2}{q^2}\mathrm{Im}\Pi_{00}}{\left[1 + \frac{G_V}{2}\mathrm{Re}\Pi_{ii} - \frac{G_V}{2}\frac{\omega^2}{q^2}\mathrm{Re}\Pi_{00}\right]^2 + \frac{G_V^2}{4}\left[\mathrm{Im}\Pi_{ii} - \frac{\omega^2}{q^2}\mathrm{Im}\Pi_{00}\right]^2}$$

$$\mathrm{Im}C'_L = \frac{\frac{\omega^2}{q^2}\mathrm{Im}\Pi_{00}}{\left[1 - G_V\left(1 - \frac{\omega^2}{q^2}\right)\mathrm{Re}\Pi_{00}\right]^2 + \left[G_V(1 - \frac{\omega^2}{q^2})\mathrm{Im}\Pi_{00}\right]^2} = \frac{\omega^2}{q^2}\mathrm{Im}C_{00}$$

[Islam *et al.*, arXiv:1411.6407]

Conserved density fluctuation in ring approximation:

- The real part of the resummed temporal correlation function:

$$\mathrm{Re}C_{00}(\omega,\vec{q}) = \frac{\mathrm{Re}\Pi_{00}(\omega,\vec{q}) + G_V\left(\frac{\omega^2}{q^2}-1\right)\left[(\mathrm{Re}\Pi_{00}(\omega,\vec{q}))^2 + (\mathrm{Im}\Pi_{00}(\omega,\vec{q}))^2\right]}{1+2G_V\left(\frac{\omega^2}{q^2}-1\right)\mathrm{Re}\Pi_{00}(\omega,\vec{q}) + \left(G_V(\frac{\omega^2}{q^2}-1)\right)^2\left[(\mathrm{Re}\Pi_{00}(\omega,\vec{q}))^2 + (\mathrm{Im}\Pi_{00}(\omega,\vec{q}))^2\right]}$$

- The resummed QNS in the ring approximation becomes:

$$\chi_q^R(T,\tilde{\mu}) = -\lim_{\vec{q}\to 0}\mathrm{Re}C_{00}(0,\vec{q}) = \frac{\chi_q(T,\tilde{\mu})}{1+G_V\chi_q(T,\tilde{\mu})}$$

Expressions for one loop vector correlator:

Temporal part:

$$\mathrm{Im}\Pi_{00}(\omega,\vec{q}) = \frac{N_f N_c}{4\pi}\int_{p_-}^{p_+} p\, dp\, \frac{4\omega E_p - 4E_p^2 - M^2}{2E_p q}\left[f(E_p-\tilde{\mu}) + f(E_p+\tilde{\mu}) - 1\right]$$

Spatial part:

$$\mathrm{Im}\Pi_{ii}(\omega,\vec{q}) = \frac{N_f N_c}{4\pi}\int_{p_-}^{p_+} p\, dp\, \frac{4\omega E_p - 4p^2 + M^2}{2E_p q}\left[f(E_p-\tilde{\mu}) + f(E_p+\tilde{\mu}) - 1\right]$$